Hindawi
Advances in Civil Engineering
Volume 2023, Article ID 4062587, 10 pages
https://doi.org/10.1155/2023/4062587

Research Article

Firefly Algorithm-Based Artificial Neural Network to Predict the Shear Strength in FRP-Reinforced Concrete Beams

Mohammad Nikoo,[1] **Babak Aminnejad**,[2] **and Alireza Lork**[3]

[1]*Department of Civil Engineering, Kish International Branch, Islamic Azad University, Kish Island, Iran*
[2]*Department of Civil Engineering, Roudehen Branch, Islamic Azad University, Roudehen, Iran*
[3]*Department of Civil Engineering, Safadasht Branch, Islamic Azad University, Tehran, Iran*

Correspondence should be addressed to Babak Aminnejad; babak.aminnejad@iau.ac.ir

Received 7 July 2022; Revised 9 January 2023; Accepted 9 February 2023; Published 21 February 2023

Academic Editor: Claudio Mazzotti

The shear strength of fiber-reinforced polymer (FRP) reinforced concrete beams is often given a large safety margin by current construction requirements. Six characteristics are utilized as inputs to compute the shear strength of FRP-reinforced concrete beams. This study uses 198 samples from the literature to predict the shear strength of 139 training samples and 59 testing samples. Additionally, the ANN structure is optimized with the firefly algorithm. The FA-ANN model is also compared to ACI-440, CSA-S806, and BISE-99 codes, and the optimized model by Nehdi et al. Findings show that regarding the shear strength of FRP-reinforced concrete beams, the firefly algorithm-optimized model performs better than the other four models. Concerning accuracy, the coefficient of correlation, R^2, was calculated as 0.961, while the average absolute error (AAE) is 0.22 for the shear strength of FRP-reinforced beams.

1. Introduction

Corrosion problems in infrastructure impose huge expenses on rehabilitating structures worldwide [1]. Furthermore, exposing structures (e.g., water treatment facilities, marine structures, and bridges) to extreme corrosion compromises their structure and, therefore, reduces their service life tremendously [2]. Fiber-reinforced polymer (FRP) bars are a promising substitute for traditional reinforcing steel bars [3, 4]. Additionally, the greater strength, smaller weight, and higher axial stiffness-to-weight ratio of FRPs make them more attractive solutions. However, FRPs suffer from a few shortcomings compared to steel, including a smaller modulus of elasticity, brittleness, and anisotropy. Recent research has focused on predicting the shear strength of FRP-reinforced concrete beams in addition to other aspects [5]. According to reports, the modulus of elasticity, shear span-to-depth ratio, beam width, concrete compressive strength, and flexural reinforcement ratio are the primary factors affecting the shear strength of FRP-reinforced concrete beams without stirrups [6].

The current shear provisions in building codes are extensions of their steel-reinforced concrete predecessors. The design codes differ significantly in their choice of influencing parameters on shear strength and their contributions. Researchers have assessed the shear provisions and concluded that they are exceedingly cautious or insufficient in some cases [5]. This overestimation results in an excess number of bars in the design, which causes reinforcing congestion and higher costs. Many provisions were devised at the time utilizing restricted experimental data [7]. The discrepancy between experimental shear test findings and code standards illuminates our lack of understanding of the shear mechanism in FRP-reinforced concrete members.

Furthermore, concrete members such as footings, slabs, and bridge decks are constructed without stirrups. In addition, sudden and brittle failure may occur in these buildings without imminent warning [3, 8]. This highlights the significance of appropriately evaluating the shear strength mechanism in FRP-reinforced concrete members [2]. Also, research has been conducted on using basalt fiber-

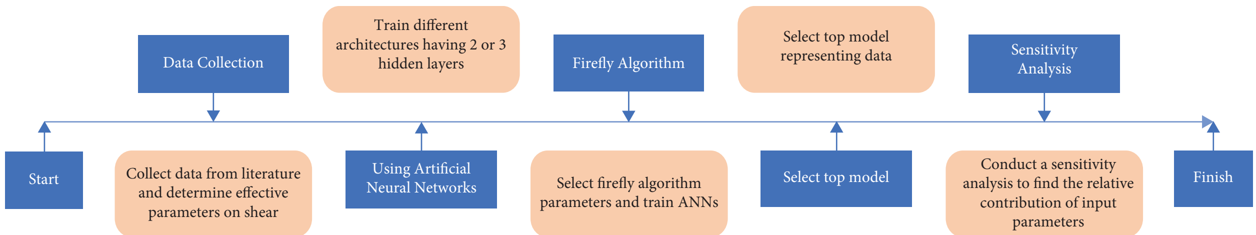

FIGURE 1: The article content outline.

reinforced polymer (BFRP) in short beams so that ten beams with a length of 2.0 meters and a rectangular section with a width of 140 mm and variable height were tested under a four-point loading configuration. Using ABAQUS software, a finite element model was established to forecast the behavior of the tested beams to a level that accurately predicted the shear capabilities of the beams and recorded their failure mechanisms [9, 10]. Also, using basalt microfibers in the fiber-reinforced polymer is a disputed topic [11], and using optimization algorithms based on ANN to determine the torsional strength of a reinforced concrete beam [12, 13].

Researchers have successfully utilized soft computing methods to increase the accuracy of shear strength prediction methods. Nehdi et al. used genetic algorithms to predict the shear strength of FRP-reinforced concrete beams [14]. Kara predicted the shear strength of FRP-reinforced beams without stirrups using genetic programming [15], while Gandomi et al. used a linear genetic programming approach for this purpose [16]. Bashir and Ashour proposed an artificial neural modeling approach, showed the feasibility of this approach, and determined the contribution of influencing factors using experimental data available at the time [17]. With more comprehensive experimental data available, Lee and Lee used the same approach for FRP-reinforced concrete beams without stirrups and proposed the relevant design equations [18]. The shear strength was predicted using a fuzzy inference technique by Nasrollahzadeh and Basiri [19]. Shahnewaz et al. optimized shear design equations using a genetic algorithm and reliability analysis for FRP-reinforced beams with stirrups [20]. Also, Golafshani and Ashour studied the feasibility of the biogeography-based optimization for FRP-reinforced concrete beams without stirrups [21]. Hasanzade-Inallu et al. estimated the shear strength of FRP-reinforced concrete beams without stirrups by amassing many experimental test results from the literature and modeling the shear strength with an ANN trained using a modified imperialist competitive optimization algorithm [7].

Several opportunities exist within these soft computing tactics to propose new models applying novel techniques to reduce model uncertainty. Yang developed the firefly algorithm, a technique for metaheuristic optimization inspired by the flashing behavior of tropical fireflies. The algorithm has successfully performed over other metaheuristic algorithms [22]. This study focused on improving the predictive accuracy of a model by training an ANN with the firefly method. The proposed method considered all the relevant factors affecting shear strength and was validated using a database of 198 specimens from the literature. The second section gives background information on ANNs and the firefly algorithm. In Section 3, the setup and training of the model are discussed. Sections 4 and 5 present the findings and conclusion, respectively. Figure 1 illustrates the organization of this study.

2. Background

2.1. Artificial Neural Networks (ANNs). ANNs were modeled based on how the human brain performs tasks and contains data processing units called neurons arranged in layers. Feedforward (FF) is a class of ANNs consisting of one input layer, one hidden layer, and one output layer. In a fully integrated FF, each layer's neurons are connected to neurons in preceding and subsequent layers. The function of a neuron is first to apply weights to its inputs to reflect the relevance of each input on the output, then add a constant called bias to the result, and then apply a function, called the activation function, to the resulting sum. The hyperbolic tangent function is a typical activation function applied for regression problems [23–25].

Typically, ANN weights are initialized randomly, causing the network's output to deviate from the desired values. A training method should modify the network weights and biases to minimize the model's error (i.e., the difference between the output and target values) [23, 24].

Training an ANN is an optimization process, and the approaches for tackling this optimization problem are divided into gradient-based and metaheuristic methods. Gradient-based techniques are fast, but they can become trapped in local minima. In contrast to gradient-based methods, metaheuristic methods are not trapped in local minima. The response provided by metaheuristic approaches is not always the global minimum. Nevertheless, these approaches often aim to explore and exploit a substantial amount of the solution space to attain the correct answers [23, 24].

ANNs are exposed to the overfitting problem. An overfitted model can reliably predict outputs for the range of inputs observed during training, but it lacks the generality necessary to predict outputs for inputs not received during training. Typically, this effect is countered by separating data into training and testing sets. The training set alters the network's weights, while the testing set is used to choose more extensible networks [24, 26].

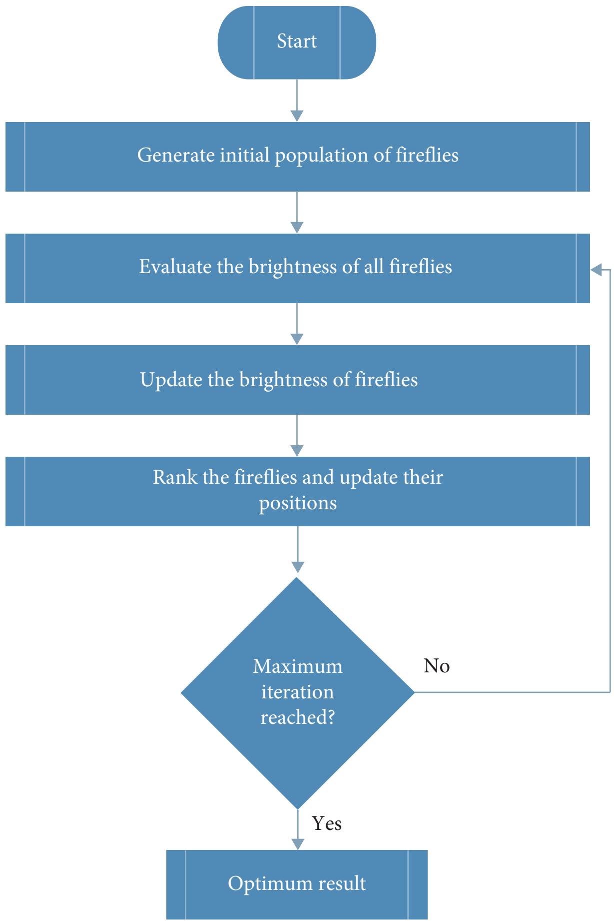

Figure 2: Flowchart of firefly algorithm.

2.2. Firefly Algorithm (FA). FA is based on the flashing pattern of tropical fireflies proposed by Yang. Researchers believe these bioluminescent signals' primary functions are to attract potential mates and prey. Also, they might act as a defensive alerting mechanism to predators. Firefly algorithm idealized this flashing behavior by using the following three simplifying assumptions:

(i) All fireflies are unisex and can absorb other fireflies regardless of gender [22].

(ii) A firefly's attractiveness is proportional to its luminosity; if two fireflies are present, the dimmer one will approach the brighter one. Due to the inverse relationship between light intensity and distance from the light source, fireflies become less attractive as their distance from the light source increases. If a firefly cannot find a firefly that is brighter than itself, it will move randomly [22].

(iii) The architecture of the objective function governs the luminance and, thus, the attractiveness of a firefly. For our implementation, the lower the cost of a firefly, the higher its brightness will be [22].

When training an ANN using the firefly algorithm, the network's weights and biases were specified as firefly locations, and the network's prediction error was defined as its cost function. As the final weights and biases of the network, the position of the firefly with the lowest cost (most brightness) was selected. Figure 2 [22, 27] shows the flowchart of the firefly algorithm.

3. Methods and Materials

3.1. Dataset. The experimental data required to train and test artificial neural networks were collected from the dataset by Hasanzade–Inallu et al. [7]. It contains 198 test cases of shear strength of FRP-reinforced concrete bars without stirrups. Table 1 provides descriptive statistics regarding the findings of the experimental test.

3.2. Model Setup. The selected parameters for training artificial neural networks (ANNs), drawn from past research, are web thickness (b_w), effective depth (d), shear span-to-depth ratio (a/d), FRP longitudinal reinforcement ratio (ρ_f), FRP bar modulus of elasticity (E_f), and concrete compressive strength (f_c'). These six parameters served as inputs to neural networks; the network's output was the shear strength.

The ANNs' input variables have varying ranges, which can increase the training time or cause the optimization algorithm to diverge [24]. Each variable was normalized to a range of [−1, 1] using the following equation to bring different input and output variables to similar ranges:

$$Y_n = \frac{2\left(Y - Y_{\min}\right)}{Y_{\max} - Y_{\text{mix}}} - 1, \quad (1)$$

where Y_n is the normalized variable value, $Y_{\max}$ is the maximum value, and $Y_{\min}$ is the minimum value. Y is the original variable value (un-normalized). Each variable's minimum and maximum values are presented in Table 1. Since the ANN will be trained using the normalized values of the variables, it is necessary to normalize any future input into a trained network and un-normalize the network's output into its original range [7].

The ANN architecture is problem-dependent [23]. The optimal architecture, including the number of neurons and hidden layers, was thus determined by trial and error (i.e., best representing the data). Forty-five architectures with two or three hidden layers were trained, and the best-performing architectures were chosen. This research used ANN models and the firefly algorithm in MATLAB software [28].

3.3. Model Training. Data were separated randomly into two groups to prevent overfitting. Seventy percent (139 test cases) were used to train the networks, while thirty percent (59 test cases) were used to test the network on data not seen during training to identify the networks with the most excellent generalization capabilities. The hyperbolic tangent function was employed as the activation function for hidden layers, while the identity function was used for the output layer.

Training a neural network aims to optimize its weights and biases (i.e., parameters) to reduce the network's prediction error. The firefly algorithm (FA) was used to train the networks. For every network architecture, the network parameters were defined as fireflies, and by generating a population of fireflies, FA

Table 1: Descriptive statistics of the experimental data [7].

	f'_c (MPa)	ρ_f (%)	E_f (GPa)	a/d	b_w (mm)	d (mm)	V_{cf} (kN)
Mean	41.57	1.07	58300	3.32	284.40	336.79	92.97
Standard deviation	13.08	0.64	42.47	1.44	190.08	210.90	112.77
Min	22.70	0.18	23.20	1.00	89.00	104.00	9.80
Max	88.30	3.43	192.00	12.50	1000.00	1097.00	953.00

Here, f'_c = concrete compressive strength; ρ_f = FRP longitudinal reinforcement ratio; E_f = FRP bar modulus of elasticity; a/d = shear span-to-depth ratio; b_w = web thickness; d = effective depth; and V_{cf} = shear strength of the concrete beam.

generated the initial possible network parameters. As the iterations of FA progressed, the network parameters (firefly positions) were updated to reflect the behavior of the training dataset and, therefore, minimize the prediction error. The final solution of the FA was chosen as the optimum network parameter for the given network architecture. The parameters chosen for FA were inspired by the recommendations given by Yang [22] and were somewhat altered to best train the ANN model. The parameters used are given in Table 2, and the description of the parameters is given in Section 2.2.

As recommended by most researchers, the chosen error measure for ANN models was the mean squared error (MSE) function given in the following equation:

$$\text{MSE} = \frac{1}{n}\sum_{i=1}^{n}\left(V_{\text{predicted},i} - V_{\text{experiment},i}\right)^2, \quad (2)$$

where n is the number of training samples (139 in our case), $V_{\text{predicted},i}$ is the neural network output for the ith sample, and $V_{\text{experiment},i}$ is the shear strength of the ith test case reported from experiments.

4. Results

4.1. Model Evaluation. Test data's mean squared error (MSE) was chosen as the error metric to select the best-performing artificial neural network (ANN) among 45 trained architectures. The top four performing ANNs are given in Table 3. The networks are sorted in the order of increasing values of the MSE value of test data. ANN identities are labeled with ANN mL (n_1-n_2-n_3), where m is the number of hidden network layers, and n_1, n_2, and n_3 are the number of neurons in the first, second, and third hidden layers, respectively.

Figure 3 provides a visual representation of the performance of the top four networks by plotting the values predicted by the networks against their experimental values from the database.

Since the points in Figure 3 are near the $y = x$ line, the projected shear strength values correspond to the observed values. Figures 4 and 5 depict the training and testing performance of the leading network, ANN 3L (2-6-2).

As demonstrated in Figures 4 and 5, the best-performing network's projected values for both the training and testing phases closely match their experimental values. It is noteworthy that the ANN 3L (2-6-2) performs well even for one test case where the shear strength is about 810 kN, which is much higher than the rest of the test cases. The ANN 3L (2-6-2) model is chosen for further analysis.

Table 2: Firefly algorithm parameters [29].

Parameter	Value
Population size	100
Mutation coefficient	0.25
Light absorption coefficient	1
Attraction coefficient base value	2
Mutation coefficient damping ratio	0.99
M (exponent of distance term)	2

4.2. Comparison with Existing Equations. ACI-440.1R-15 [30], CAN/CSA-S806-12 [31], BISE-99 [32], and Nehdi et al. (optimized equation method) provide the shear design requirements for FRE-reinforced concrete beams without stirrups.) [33, 34]. Thus, they were used on experimental test data. Their predictions were calculated to evaluate the relative accuracy of the selected ANN 3L (2-6-2) model compared to other models recommended by code provisions and some published models (strength reduction coefficient assumed to be $\varphi = 1$). For a visual indication of the accuracy of equations given by ACI-440.1R-15 [30], CAN/CSA-S806-12 [31], BISE-99 [32], and the optimized equation by Nehdi et al. [14, 33], their predictive values are plotted against the experimental values and are illustrated in Figure 6. The three considered codes underestimate the shear strength, confirming the reports from other researchers [7, 17].

In addition, the mean, standard deviation (SD), and coefficient of variation (CV) of the equations' forecasted shear resistance were assessed. The values provided by the top four ANN models are given in Table 4. The model is considered accurate when the mean value is near one and SD returns a low value. Compared to other ANN models, although ANN 3L (2-6-2) does not have a mean value closest to one, it is identified as the best model since its CV value is the lowest. Therefore, the model's statistics are more reliable. The model's coefficient of variation (R^2) is also calculated and depicted in Figure 7. The ANN 3L (2-6-2) model has the most significant variation coefficient, and best describes the variation in the data.

The Taylor diagram (Figure 8) provides an additional visual comparison of the performance of the FA-ANN model and that of the other code models. It presents a graphical representation of each model's applicability based on the root mean square-centered difference, correlation coefficient, and standard deviation. The results of the study indicate that the FA-ANN model better estimates the total deflection closest to the experimental

Table 3: Top four ANN statistics.

Num	Topology	Train				Test			
		R^2	$y = ax + b$	RMSE	AAE	R^2	$y = ax + b$	RMSE	AAE
1	FA-ANN 3L (2-6-2)	0.972	$y = 0.9426x + 3.9394$	20.18	0.21	0.952	$y = 1.0783x + 0.9683$	26.37	0.25
2	FA-ANN 3L (8-2-4)	0.970	$y = 0.9554x + 3.9683$	20.37	0.24	0.942	$y = 1.1022x + 1.6858$	30.98	0.32
3	FA-ANN 3L (3-7-3)	0.955	$y = 0.9303x + 5.0749$	25.14	0.26	0.928	$y = 1.1101x - 0.4873$	33.84	0.30
4	FA-ANN 3L (3-8-2)	0.965	$y = 0.9696x + 2.8502$	21.95	0.25	0.943	$y = 1.1669x - 4.1261$	34.73	0.31

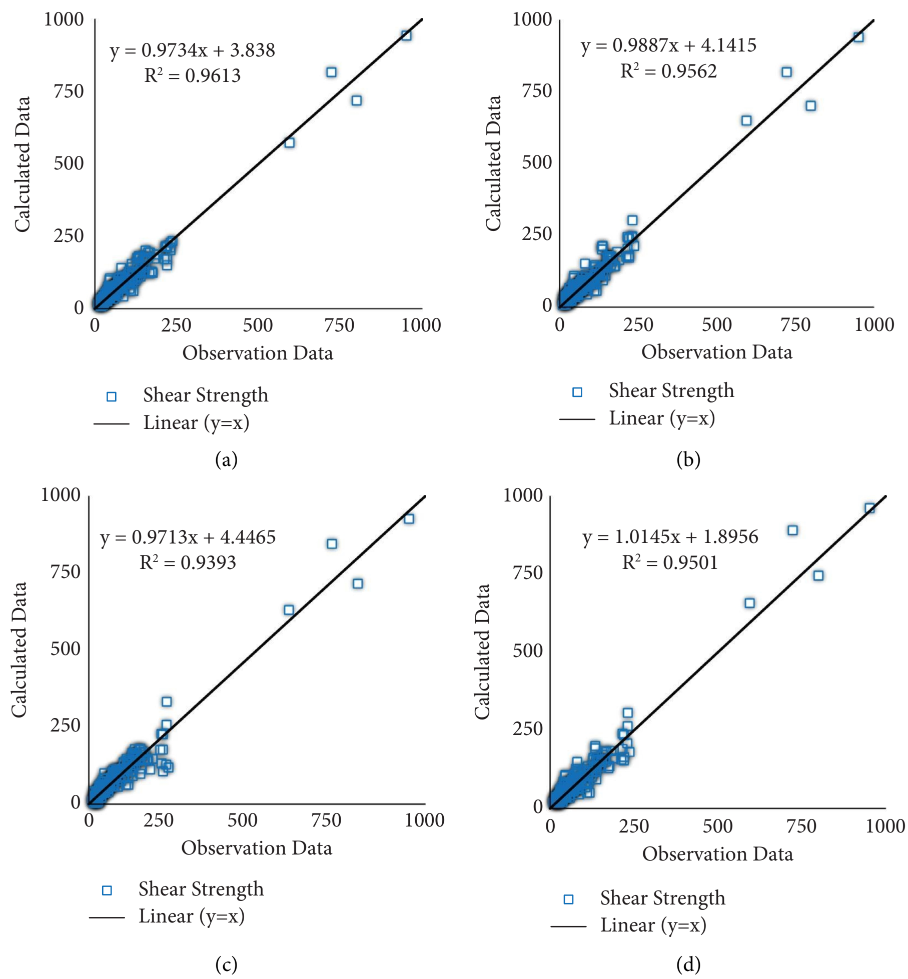

Figure 3: Experimental vs. predicted values of shear strength for (a) ANN 3L (2-6-2) model, (b) ANN 3L (8-2-4), (c) ANN 3L (3-7-3) model, and (d) ANN 3L (3-8-2) model.

shear strength of FRP-reinforced beams, followed by the model developed by Nehdi et al. Compared to the ACI-440 and BISE-99 code models, the CSA-S806 model produced higher root mean square-centered difference and SD values, indicating a model with less precision when approximating experimental data.

4.3. Sensitivity Analysis. A sensitivity analysis determined the effect of inputs on the outputs [35]. In this work, the Gevrey et al. [35, 36] profile approach was implemented in MATLAB software [28]. This technique evaluates each input variable individually while keeping the others constant. During execution, the scale separated the range of each input variable into many equal intervals. The remaining variables were assigned to n distinct constant values, and the network output was calculated across the whole range of the chosen variable, resulting in n distinct output groups. Finding the median output for each input scenario was the last step in combining the n output groups. The minimum, first quartile, median, third quartile, and maximum were utilized as constant values for each variable. Lek offers the details of the method [35, 36]. The chosen scale was 192, as suggested by Gevrey et al. [35, 36].

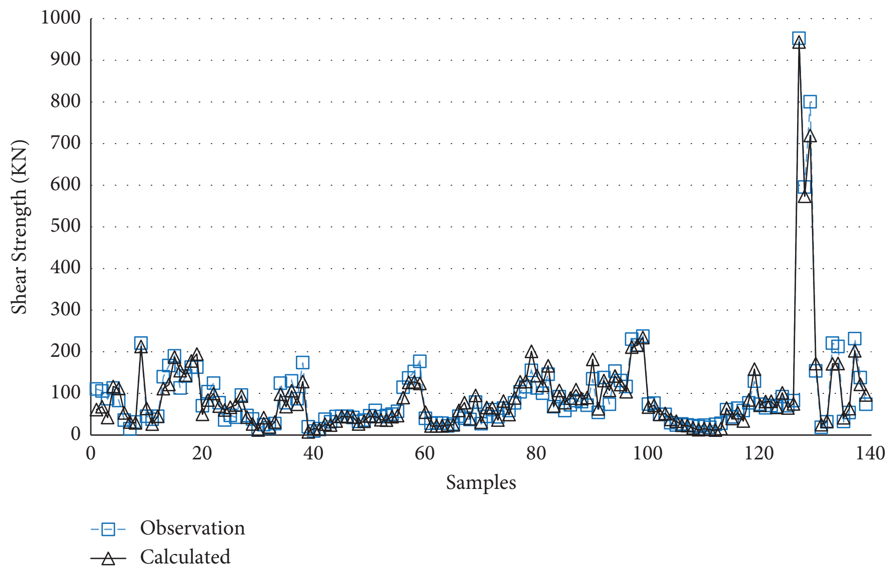

FIGURE 4: Comparison between ANN 3L (2-6-2) calculated and observation data used in training.

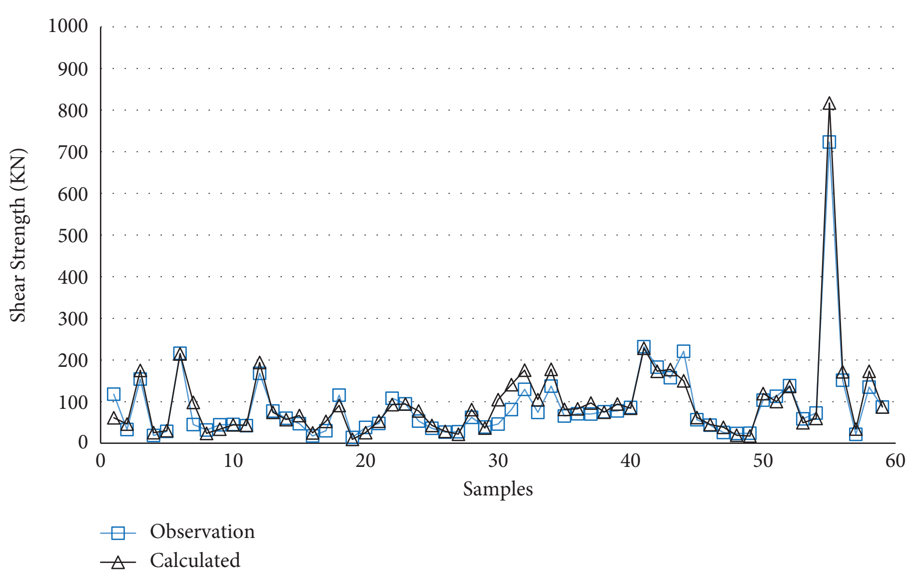

FIGURE 5: Comparison between ANN 3L (2-6-2) calculated and observation data used in testing.

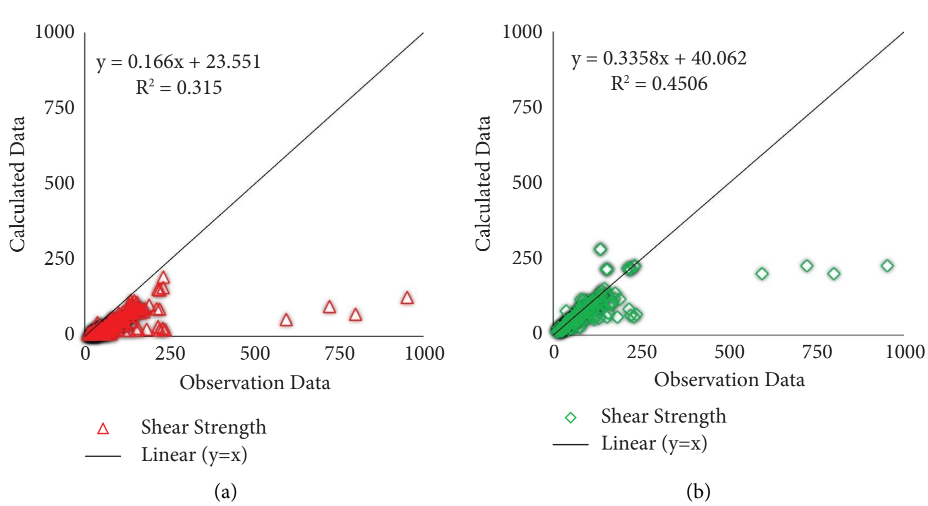

FIGURE 6: Continued.

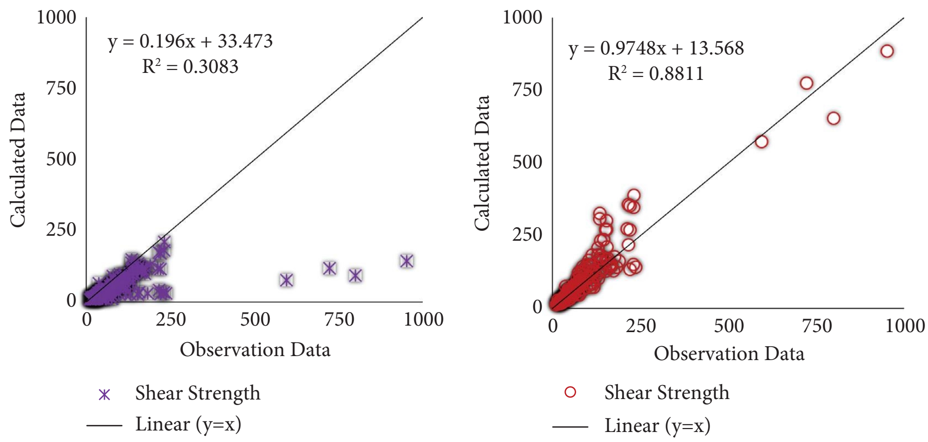

(c) (d)

FIGURE 6: Experimental vs. predicted values of shear strength for (a) ACI-440.1R-15 equation, (b) CSA-S806-12 equation, (c) BISE-99 equation, and (d) Nehdi et al. (optimized) equation.

TABLE 4: Statistical index of experimental to the predicted shear strength of FRP-reinforced beams.

Num	Topology	All			
		R^2	$y = ax + b$	RMSE	AAE
1	FA-ANN 3L (2-6-2)	0.961	$y = 0.9734x + 3.838$	22.21	0.22
2	FA-ANN 3L (8-2-4)	0.956	$y = 0.9887x + 4.1415$	24.03	0.26
3	FA-ANN 3L (3-7-3)	0.939	$y = 0.9713x + 4.4465$	28.02	0.27
4	FA-ANN 3L (3-8-2)	0.950	$y = 1.0145x + 1.8956$	26.41	0.27
5	ACI-440	0.315	$y = 0.166x + 23.551$	111.69	0.53
6	CSA-S806	0.451	$y = 0.3358x + 40.062$	88.28	0.22
7	BISE-99	0.308	$y = 0.196x + 33.473$	104.76	0.36
8	Nehdi et al	0.881	$y = 0.9748x + 13.568$	41.91	0.25

Figure 9 depicts the explanatory variables' relative influence and contribution (six inputs) on the response variable (shear strength).

The two most essential criteria are beam width and effective depth. Since average stress equals shear force divided by cross-sectional area, width increase directly affects shear strength. Since higher effective depth results in longer diagonal shear cracks at maximum loading, beams with greater effective depth have greater shear strength. Shear strength has the most negligible effect on concrete compressive strength.

4.4. Predictive Model and ANN Weights. Since the generated ANN 3L (2-6-2) would be useless without its source file, the weights and biases of the trained network are given in this study. The input data must be normalized with equation (1) using the minimum and maximum values from Table 1, and the output from the network must be denormalized using equation (3). The input is the 6×1 vector, $\mathbf{a}^{(1)}$. The shear strength is determined by the following equations [7, 37]:

$$\begin{aligned}
\mathbf{a}^{(2)} &= \tan h\left(\vartheta^{(1)} \times \mathbf{a}^{(1)} + \mathbf{b}_1\right),\\
\mathbf{a}^{(3)} &= \tan h\left(\vartheta^{(2)} \times \mathbf{a}^{(2)} + \mathbf{b}_2\right),\\
\mathbf{a}^{(4)} &= \tan h\left(\vartheta^{(3)} \times \mathbf{a}^{(3)} + \mathbf{b}_3\right),\\
V_c^{\text{predict (normalized)}} &= \tan h\left(\vartheta^{(4)} \times \mathbf{a}^{(4)} + b_4\right),\\
V_c^{\text{predict}} &= \frac{V_c^{\text{predict (normalized)}} + 1}{2} \times \left(V_{\max} - V_{\min}\right) + V_{\min},
\end{aligned} \tag{3}$$

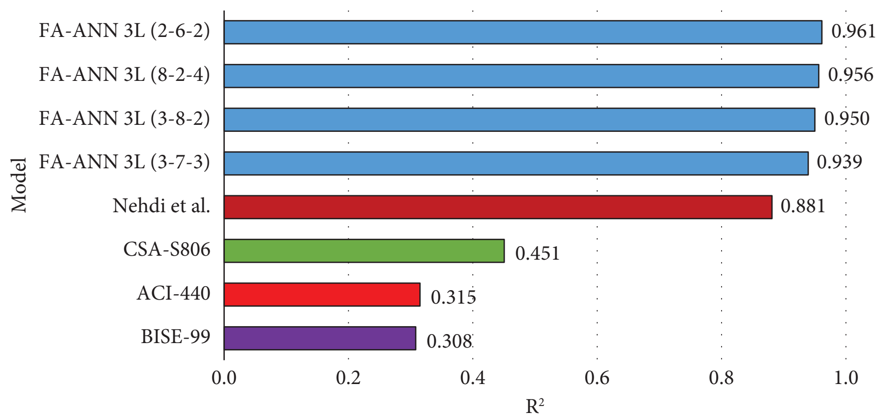

Figure 7: Coefficient of determination values for ANN models, multiple regression models, and models published in literature and codes.

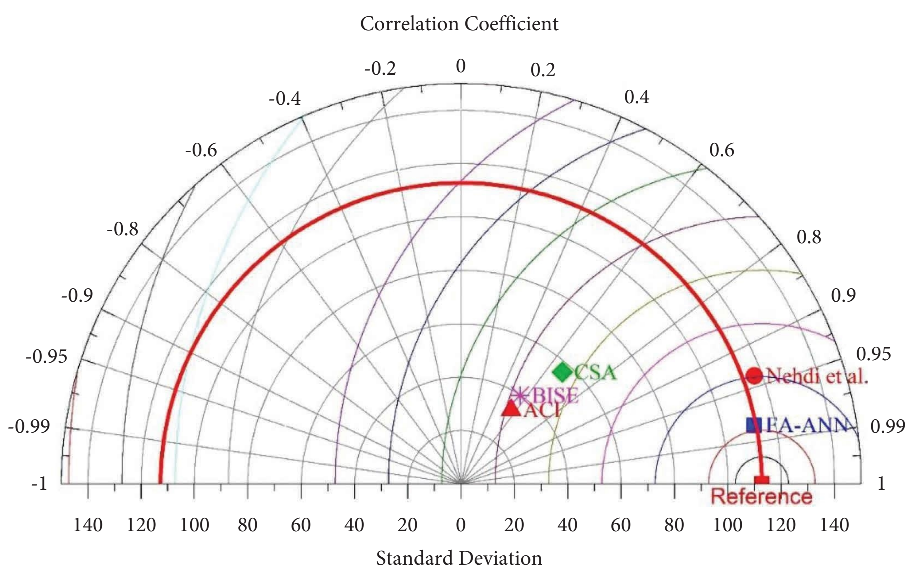

Figure 8: Taylor diagram depiction of the various models' projections.

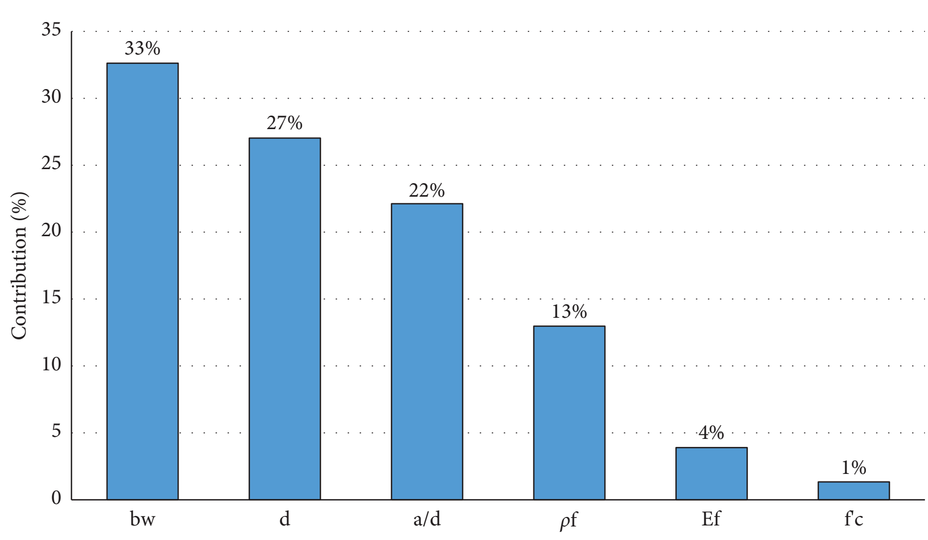

Figure 9: Relative contribution of six input parameters to the prediction of shear strength.

where $\tanh$ = hyperbolic tangent function; V_c^{predict} = predicted value of shear strength, and $V_{\max}$ and $V_{\min}$ = minimum and maximum shear strengths provided in Table 1. The weight (θ) and bias (b) matrices are provided in the following:

$$
\begin{aligned}
\vartheta^{(1)} &= 10^{-1}\times\begin{bmatrix} 2.2164 & -0.6883 & 8.6643 & -10.0000 & -9.9421 & 3.3755 \\ 0.2448 & -2.8990 & 2.6792 & 10.0000 & -8.3346 & -2.2653 \end{bmatrix},\\
\vartheta^{(2)} &= 10^{-1}\times\begin{bmatrix} -10.0000 & 6.0145 & 6.7892 & -4.3231 & 2.1742 & 8.7769 \\ 8.3649 & 8.6428 & -6.4922 & -9.6582 & -5.2643 & -10.0000 \end{bmatrix}^{T},\\
\vartheta^{(3)} &= 10^{-1}\times\begin{bmatrix} -3.9723 & -5.3190 & 7.2372 & 4.0631 & -0.6853 & 6.1589 \\ 8.4195 & -4.6722 & -9.4349 & -7.1096 & -2.5752 & -6.2628 \end{bmatrix},\\
\vartheta^{(4)} &= 10^{-1}\times\begin{bmatrix} 9.5694 & -8.6457 \end{bmatrix},\\
\mathbf{b}_1 &= 10^{-1}\times\begin{bmatrix} -3.2927 & 7.0137 \end{bmatrix}^{T},\\
\mathbf{b}_2 &= 10^{-1}\times\begin{bmatrix} 9.8089 & -2.7279 & -9.9623 & 9.1751 & -3.7018 & -9.3895 \end{bmatrix}^{T},\\
\mathbf{b}_3 &= 10^{-1}\times\begin{bmatrix} 1.2541 & -7.1203 \end{bmatrix}^{T},\\
\mathbf{b}_4 &= 0.6549.
\end{aligned}
\tag{4}
$$

5. Conclusion

One hundred ninety-eight published experimental test results were compiled to solve the fiber-reinforced polymer (FRP) reinforced concrete beam shear strength prediction problem with longitudinal bars and without stirrups. The firefly algorithm (FA) was used to train the ANN models. The results analysis suggests the following:

(1) The trained FA-ANN 3L model (2-6-2) is more accurate than other ANNs with similar topologies for estimating concrete beam shear strength. This model's RMSE and AAE for all available data were 22.21 and 0.22, respectively.

(2) Nehdi et al. introduced a straightforward experimental model for estimating the shear strength of concrete beams. It offered acceptable results; however, these results are less accurate than the proposed FA-ANN 3L (2-6-2) model.

(3) The trained ANN 3L (2-6-2) model can predict the shear strength more accurately than the three code provisions and two models suggested in the literature. The mean value and standard deviation of experimental to predicted values are 1.0342 and 0.3073, respectively.

(4) According to the sensitivity analysis results, the beam width and effective depth are the most influential parameters on the shear strength of FRP-reinforced beams. The least influential factor is concrete compressive strength.

(5) Based on the weights and biases of the ANN 3L (2-6-2) model (top-trained model), a predictive model was developed to enable access to the trained model without the source file.

(6) Findings confirm literature concerns that code standards underestimate the shear strength of FRP-reinforced concrete beams, which could increase costs and reinforce bar congestion.

Data Availability

The datasets are available in the Appendix at https://link.springer.com/article/10.1007/s11771-019-4243-z, and researchers can access to datasets.

Conflicts of Interest

The authors declare that they have no conflicts of interest.

References

[1] G. B. Jumaa and A. R. Yousif, "Size effect on the shear failure of high-strength concrete beams reinforced with basalt FRP bars and stirrups," *Construction and Building Materials*, vol. 209, pp. 77–94, 2019.

[2] M. K. Dhahir and W. Nadir, "A compression field based model to assess the shear strength of concrete beams reinforced with longitudinal FRP bars," *Construction and Building Materials*, 2018.

[3] A. Dev, M. Chellapandian, S. S. Prakash, and Y. Kawasaki, "Failure-mode analysis of macro-synthetic and hybrid fibre-reinforced concrete beams with GFRP bars using acoustic emission technique," *Construction and Building Materials*, 2020.

[4] H. Naderpour, O. Poursaeidi, and M. Ahmadi, "Shear resistance prediction of concrete beams reinforced by FRP bars using artificial neural networks," *Measurement*, vol. 126, pp. 299–308, 2018.

[5] K. Nasrollahzadeh and R. Aghamohammadi, "Reliability analysis of shear strength provisions for FRP-reinforced concrete beams," *Engineering Structures*, vol. 176, pp. 785–800, 2018.

[6] G. B. Jumaa and A. R. Yousif, "Size effect in shear failure of high strength concrete beams without stirrup reinforced with basalt FRP bars," *KSCE Journal of Civil Engineering*, vol. 23, no. 4, pp. 1636–1650, 2019.
[7] A. Hasanzade-Inallu, P. Zarfam, and M. Nikoo, "Modified imperialist competitive algorithm-based neural network to determine shear strength of concrete beams reinforced with FRP," *Journal of Central South University*, vol. 26, no. 11, pp. 3156–3174, 2019.
[8] M. Kaszubska, R. Kotynia, and J. A. O. Barros, "Influence of longitudinal GFRP reinforcement ratio on shear capacity of concrete beams without stirrups," *Procedia Engineering*, vol. 193, pp. 361–368, 2017.
[9] F. Abed, A. El Refai, and S. Abdalla, "Experimental and finite element investigation of the shear performance of BFRP-RC short beams," *Structures*, vol. 20, pp. 689–701, 2019.
[10] A. El Refai and F. Abed, "Concrete contribution to shear strength of beams reinforced with basalt fiber-reinforced bars," *Journal of Composites for Construction*, vol. 20, no. 4, Article ID 4015082, 2016.
[11] F. Abed, M. K. Sabbagh, and A. S. Karzad, "Effect of basalt microfibers on the shear response of short concrete beams reinforced with BFRP bars," *Composite Structures*, vol. 269, Article ID 114029, 2021.
[12] Z. Lyu, Y. Yu, B. Samali et al., "Back-propagation neural network optimized by K-fold cross-validation for prediction of torsional strength of reinforced concrete beam," *Materials*, vol. 15, no. 4, p. 1477, 2022.
[13] Y. Yu, S. Liang, B. Samali et al., "Torsional capacity evaluation of RC beams using an improved bird swarm algorithm optimised 2D convolutional neural network," *Engineering Structures*, vol. 273, Article ID 115066, 2022.
[14] M. Nehdi, H. El Chabib, and A. A. Saïd, "Proposed shear design equations for FRP-reinforced concrete beams based on genetic algorithms approach," *Journal of Materials in Civil Engineering*, vol. 19, no. 12, pp. 1033–1042, 2007.
[15] I. F. Kara, "Prediction of shear strength of FRP-reinforced concrete beams without stirrups based on genetic programming," *Advances in Engineering Software*, vol. 42, no. 6, pp. 295–304, 2011.
[16] A. H. Gandomi, D. Mohammadzadeh S, J. L. Pérez-Ordóñez, and A. H. Alavi, "Linear genetic programming for shear strength prediction of reinforced concrete beams without stirrups," *Applied Soft Computing*, vol. 19, pp. 112–120, 2014.
[17] R. Bashir and A. Ashour, "Neural network modelling for shear strength of concrete members reinforced with FRP bars," *Composites Part B: Engineering*, vol. 43, no. 8, pp. 3198–3207, 2012.
[18] S. Lee and C. Lee, "Prediction of shear strength of FRP-reinforced concrete flexural members without stirrups using artificial neural networks," *Engineering Structures*, vol. 61, pp. 99–112, 2014.
[19] K. Nasrollahzadeh and M. M. Basiri, "Prediction of shear strength of FRP reinforced concrete beams using fuzzy inference system," *Expert Systems with Applications*, vol. 41, no. 4, pp. 1006–1020, 2014.
[20] M. Shahnewaz, R. Machial, M. S. Alam, and A. Rteil, "Optimized shear design equation for slender concrete beams reinforced with FRP bars and stirrups using Genetic Algorithm and reliability analysis," *Engineering Structures*, vol. 107, pp. 151–165, 2016.
[21] E. M. Golafshani and A. Ashour, "A feasibility study of BBP for predicting shear capacity of FRP reinforced concrete beams without stirrups," *Advances in Engineering Software*, vol. 97, pp. 29–39, 2016.
[22] X. S. Yang, *Nature-Inspired Optimization Algorithms*Elsevier Science, Amsterdam, The Netherlands, 2014.
[23] A. Géron, *Hands-on Machine Learning with Scikit-Learn and TensorFlow: Concepts, Tools, and Techniques to Build Intelligent Systems*, O'Reilly Media, Inc, Sebastopol, CA, USA, 2017.
[24] S. Haykin, *Neural Networks and Learning Machines*Vol. 3, Pearson Education India, Noida, India, 2008.
[25] M. M. Nikoo, M. Hadzima-Nyarko, E. Karlo Nyarko, M. M. Nikoo, E. Karlo Nyarko, and M. M. Nikoo, "Determining the natural frequency of cantilever beams using ANN and heuristic search," *Applied Artificial Intelligence*, vol. 32, no. 3, pp. 309–334, 2018.
[26] M. Nikoo, L. Sadowski, F. Khademi, and M. Nikoo, "Determination of damage in reinforced concrete frames with shear walls using self-organizing feature map," *Applied Computational Intelligence and Soft Computing*, vol. 2017, Article ID 3508189, 10 pages, 2017.
[27] I. Fister, M. Perc, S. M. Kamal, and I. Fister, "A review of chaos-based firefly algorithms: perspectives and research challenges," *Applied Mathematics and Computation*, vol. 252, pp. 155–165, 2015.
[28] Matlab, "MATLAB-Mathworks," 2018, https://in.mathworks.com/products/matlab.html.
[29] I. Faridmehr, M. L. Nehdi, M. Nikoo, and K. A. Valerievich, "Predicting embodied carbon and cost effectiveness of post-tensioned slabs using novel hybrid firefly ANN," *Sustainability*, vol. 13, no. 21, Article ID 12319, 2021.
[30] A. Committee, "Guide for the design and construction of structural concrete reinforced with FRP bars," American Concrete Institute, Michigan, USA, Aci 440.1R-15, 2015.
[31] Can/Csa, *CAN/CSA-S806-12. Design and Construction of Building Structures with Fibre-Reinforced Polymers*, Canadian Standards Association, Ontario, Canada, 2012.
[32] IstructE, *Interim Guidance on the Design of Reinforced concrete Structures Using Fibre Composite Reinforcement*, Institution of Structural Engineers (IStructE), SETO Ltd, London, UK, 1999.
[33] R. Machial, M. S. Alam, and A. Rteil, "Revisiting the shear design equations for concrete beams reinforced with FRP rebar and stirrup," *Materials and Structures*, vol. 45, no. 11, pp. 1593–1612, 2012.
[34] M. Nehdi and H. Nikopour, "Genetic algorithm model for shear capacity of RC beams reinforced with externally bonded FRP," *Materials and Structures*, vol. 44, no. 7, pp. 1249–1258, 2011.
[35] M. Gevrey, I. Dimopoulos, and S. Lek, "Review and comparison of methods to study the contribution of variables in artificial neural network models," *Ecological Modelling*, vol. 160, no. 3, pp. 249–264, 2003.
[36] S. Lek, M. Delacoste, P. Baran, I. Dimopoulos, J. Lauga, and S. Aulagnier, "Application of neural networks to modelling nonlinear relationships in ecology," *Ecological Modelling*, vol. 90, no. 1, pp. 39–52, 1996.
[37] A. Andalib, B. Aminnejad, and A. Lork, "Grey wolf optimizer-based ANNs to predict the compressive strength of self-compacting concrete," *Applied Computational Intelligence and Soft Computing*, vol. 2022, Article ID 9887803, 17 pages, 2022.